Catalysis Letters, Vol. 115, Nos. 3–4, June 2007 (© 2007)
DOI: 10.1007/s10562-007-9079-8

Direct synthesis and superior catalytic performance of V-containing SBA-15 mesoporous materials for oxidative dehydrogenation of propane

Fang Ying, Jianhui Li, Chuanjing Huang,* Weizheng Weng, and Huilin Wan*

Department of Chemistry, The State Key Laboratory for Physical Chemistry of Solid Surfaces, Xiamen University, Xiamen, 361005, P.R. China

Received 6 March 2007; accepted 6 March 2007

V-containing SBA-15 mesoporous materials have been directly synthesized in an acidic and peroxidic medium. Compared to V/SBA-15 and V/SiO_2 samples prepared by impregnation method, the materials thus synthesized show larger surface areas, higher dispersion and reducibility of VO_x species, and superior catalytic performance for oxidative dehydrogenation of propane.

KEY WORDS: V-containing SBA-15 mesoporous materials; preparation; oxidative dehydrogenation of propane.

1. Introduction

The discovery and improvement of heterogeneous catalysts active for the oxidative dehydrogenation (ODH) of light alkanes remains as a particularly challenging matter in catalysis research. Extensive studies have been made on supported vanadium oxides [1–5]. It has been established that the catalytic behaviour is related to parameters such as the oxidation state, coordination number, aggregation state and reducibility of vanadium species. These parameters are influenced not only by the V loading but also by the nature of support and the preparation of catalyst. Liu et al. [6] have recently prepared highly efficient VO_x/SBA-15 catalysts for ODH of propane by alcoholic impregnation method. The results demonstrated that, being a carrier of supported vanadium oxide catalysts for the reaction, SBA-15 is superior to MCM-41 and SiO_2.

SBA-15, a mesoporous hexagonal silica with large pores, thick walls and high hydrothermal stability may be used as a promising catalyst support. Furthermore, its large internal surface area allows for the dispersion of a large number of catalytically active centers. Although of great potential use for catalytic applications, there have been only a few reports on the post-synthesis of SBA-15 supported vanadium oxide using grafting/anion-exchange and various impregnation methods [6–9]. To our knowledge, no studies have been made on the direct synthesis of V-containing SBA-15 mesoporous silica.

*To whom correspondence should be addressed.
E-mails: huangcj@xmu.edu.cn; hlwan@xmu.edu.cn

Recently, Briot et al. have reported the direct (one-pot) synthesis of Mo-containing SBA-15 in an acidic and peroxidic medium [10, 11]. In this work, we report for the first time the direct synthesis of V-containing SBA-15 by the peroxo route. The mesoporous structure and the nature of vanadium oxide are characterized by XRD, N_2 adsorption, laser Raman spectroscopy and TPR techniques. The catalytic performances of thus synthesized catalysts for ODH of propane are tested and compared with that prepared by impregnation method.

2. Experimental

2.1. Catalyst preparation

The V-containing SBA-15, denoted as V-SBA-15, was synthesized in a similar manner as reported for Mo-SBA-15 [10] with slight modifications. Typically, 4 g of $EO_{20}PO_{70}EO_{20}$ and 0.227 g of CTMACl were dissolved in 150 mL of aqueous HCl (2 mol/L) to prepare solution A; a desired amount of V_2O_5, 30% H_2O_2 and H_2O (molecular ratio: $H_2O_2/V(V)/H_2O$ = 1.7/0.06/106) were mixed at 60 °C to form a deep orange solution of oxo-peroxo vanadium species (solution B). 9.1 mL of TEOS was added to solution A and then mixed with cooled solution B, followed by moderate stirring for 4 h at room temperature, filtration, repeated washing with distilled water, drying overnight and calcination at 500 °C for 6 h.

For comparison, SBA-15- and SiO_2-supported V catalysts were also prepared by impregnation method. The support, SAB-15, was synthesized according to the literature procedure [12]. Briefly, a homogeneous

mixture comprised of $EO_{20}PO_{70}EO_{20}$ and TEOS in hydrochloric acid was stirred at 40 °C for 24 h and further treated at 95 °C for 24 h. The solid products were recovered by filtration and calcined at 550 °C for 6 h. The thus synthesized SBA-15 or SiO_2 was impregnated with an aqueous solution of NH_4VO_3, followed by drying and calcining at 500°C for 6 h. The resulted materials were denoted as V/SBA-15 and V/SiO_2, respectively.

2.2. Catalyst characterization

X-ray diffraction (XRD) patterns were recorded on a Rigaku Rotaflex D/max-C X-ray power diffractometer with Cu Kα radiation. N_2 adsorption and desorption isotherms were recorded on an automated Micromeritics Tri-Star 3000 apparatus. High-resolution transmission electron microscopy (HRTEM) was performed on a TECNAI 30 G2 instrument equipped with an EDX LINK-ISIS accessory. *In situ* laser Raman spectroscopy (LRS) were measured using Renishaw UV-Vis Raman 1000 System equipped with a CCD detector and a Leica DMLM microscope. The line at 514.5 nm of an Ar^+ laser was used for excitation. The sample wafer was placed in a high-temperature *in situ* Raman cell designed for microprobe LRS. The spectra were recorded in O_2 flow at 500 ° C. H_2-TPR was performed on a flow apparatus using a 5% H_2/Ar mixture flowing at 20 mL/min. The heating rate was 10 °C. Hydrogen consumption was monitored by a TCD detector after removing the water formed.

2.3. Catalytic reaction

The selective oxidation of propane was carried out in a fixed bed flow reactor under atmospheric pressure. 0.133 g of catalyst was loaded in a quartz tubular reactor (5-mm i.d.). The remaining space of the reactor was filled with quartz sand to minimize possible homogeneous reaction. The molar composition of the reactant gas was C_3H_8:O_2:He = 1.2:1.0: 1.2. The product was analyzed by on-line gas chromatography.

3. Results and discussion

3.1. Catalyst characterization

The results from ICP analysis and N_2-adsorption measurements are listed in Table 1. Significantly higher surface areas are observed for V-SBA-15 samples, although their pore volume and pore diameter values are lower than that of V/SBA-15 and V/SiO_2. No tendency is observed in the change of surface area with the introduction of V into SBA-15 by the direct synthesis, except that V content increases up to 3.4%. On the other hand, V/SBA-15 samples present a decrease in their surface areas due to V introduction by impregnation method.

All the V-SBA-15 samples present almost the same XRD pattern and N_2 adsorption–desorption isotherm. As shown in figure 1, 3V-SBA-15 shows one intense diffraction indexed to (100) pane and two weak diffraction peaks corresponding to (110) and (200) planes. This pattern is similar to that of pure SBA-15 and assigned to an ordered hexagonal structure. Compared to SBA-15, the higher order (110) and (200) diffractions become less resolved, showing a slight decease in mesopore ordering with 3V-SBA-15. This phenomenon could be explained by the fact that no hydrothermal treatment was used during the synthesis procedure [10]. From figure 1, it is also seen that the N_2 adsorption–desorption isotherm of 3V-SBA-15 shows a sharp step with a hysteresis loop corresponding to the filling of ordered mesopores. That hexagonal mesostructure is further confirmed by the HRTEM images as shown in figure 2. The micrographs show well-defined mesoporous structures, suggesting a hexagonal arrangement of the mesophase.

Figure 3 shows the Raman spectra of V-SBA-15 and V/SBA-15 catalysts. All the samples present Raman bands at 492, 608 and 1032 cm^{-1}. The bands at 492 and 608 cm^{-1} originate from tri- and tetra-cyclosiloxane rings of the SBA-15 support, respectively [13]. The sharp band at 1032 cm^{-1} is characteristic of the V=O stretching vibration of tetrahedral VO_4 species, which

Table 1
Physical properties of various samples

Samples	Preparation method[a]	Si/V ratio in preparation	Si/V ratio By ICP	V-content		S_{BET} (m^2/g)	V_p (cm^3/g)	r_p (nm)
				V/Si (at.%)	(wt.%)			
Pure SBA-15	HTS	–	–	0	0	710	0.95	5.4
0.8V-SBA-15	DPS	50	125	0.8	0.7	915	0.85	5.4
1.8V-SBA-15	DPS	29	56	1.8	1.5	887	0.74	4.3
3V-SBA-15	DPS	18	33	3.0	2.5	908	0.75	4.9
3.4V-SBA-15	DPS	9	29	3.4	2.8	725	0.68	5.1
1V/SBA-15	IMP	100	n.d	1.0	0.8	582	0.95	7.6
1.8V/SBA-15	IMP	56	n.d	1.8	1.5	554	0.92	7.3
3V/SBA-15	IMP	33	n.d	3.0	2.5	531	0.80	6.9
3V/SiO_2	IMP	33	n.d	3.0	2.5	245	0.74	11.5

[a] HTS, hydrothermal synthesis as described in reference [12]; DPS, direct peroxo-route synthesis; IMP, impregnation.

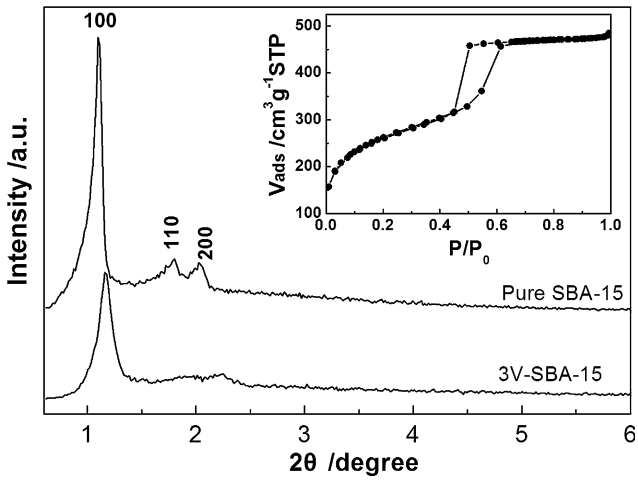

Fig. 1 XRD patterns of SBA-15 and 3V-SBA-15 samples. The inset shows the N_2 sorption isotherm of the 3V-SBA-15.

are isolated and bound directly to the silica [14, 15]. Although 1.8V/SBA-15 presents only Raman features assigned to SBA-15 and isolated VO_4 species, 3V/SBA-15 shows spatial inhomogeneity in the spectral appearance. This is evidenced by the typical Raman spectra (spectrum b and c) of 3V/SBA-15 recorded at different spots. In the spectrum c, several additional bands appear at 142, 282, 406 and 990 cm^{-1}, which are indicative of microcrystalline V_2O_5 particles [16]. On V-SBA-15 catalysts, a weak band is observed at 965 cm^{-1}. A band near 960 cm^{-1} has been previously observed in the spectra of V-substituted silicalites and has been assigned to the stretching vibration modes of the $[\equiv Si\text{-}O]^{\delta-}$ unit perturbed by the presence of V [17]. Thus, it is likely that a part of vanadium may be incorporated into the framework by the direct synthesis in this work. However, the majority of the vanadia species is present as the isolated VO_4 species, because the 1032-cm^{-1} band is much stronger than the band at 965 cm^{-1}. In addition, no bands due to V–O–V bonds could be observed for V-SBA-15 samples in spite of V content increasing up to 3.4 at.%, indicating a high dispersion of VO_x species.

H_2-TPR results are shown in figure 4, where the temperatures of reduction peaks (T_{max}) are indicated. The T_{max} values provide the following reducibility scale: V-SBA-15 > V/SBA-15 > V/SiO_2. When the content of V is increased from 1.8 to 3 at.%, the T_{max} value of V-SBA-15 remains almost unchanged, while that of V/SBA-15 shifts to higher temperature. Furthermore, on 3V/SBA-15 two weak peaks appear at 658 and 682 °C. Many studies have revealed that the reducibility of supported V oxide is relative to its structure and dispersion. The peaks at low temperatures (ca. 540 °C) are attributable to the reduction of isolated tetrahedral vanadium species, while the peaks at 658 and 682 ° C could be ascribed to V_2O_5-like species [18]. It is likely that on V/SBA-15 and V/SiO_2 catalysts some polymeric V species, i.e. $(VO_x)_n$ could be formed. This could account for their higher reduction temperatures as compared with V-SBA-15 catalysts. In the case of V/SBA-15, the shift of reduction peak with increasing V content suggests a progressive formation of less reducible higher polymeric V species. In contrast, the TPR behaviour of V-SBA-15 indicates a high dispersion of V species in the catalyst, which is in agreement with the above Raman results.

3.2. Catalytic performance

The superior catalytic performance of the V-SBA-15 mesoporous materials can be seen from Table 2. Blank results show that negligible homogenous reaction could occur under the reaction conditions used here, due to the remaining space of the reactor was filled with quartz sand, as described in the Experimental section. The products on all the catalysts studied are mainly C_3H_6 and CO_x (CO and CO_2), accompanied by small amounts of C_2H_4, CH_4 and oxygenates. Propane conversion and propylene yield on V-SBA-15 catalysts increase sharply with V content, and attain maximum values at 1.8∼

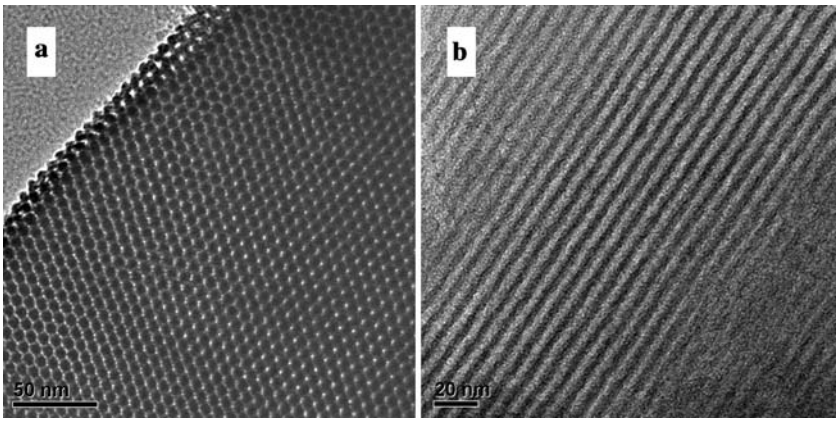

Fig. 2 (**a**) HRTEM images of 3V-SBA-15 with the electron beam parallel (a) and perpendicular (b) to the pore direction. (**b**) HRTEM images of 3V-SBA-15 with the electron beam parallel (a) and perpendicular (b) to the pore direction.

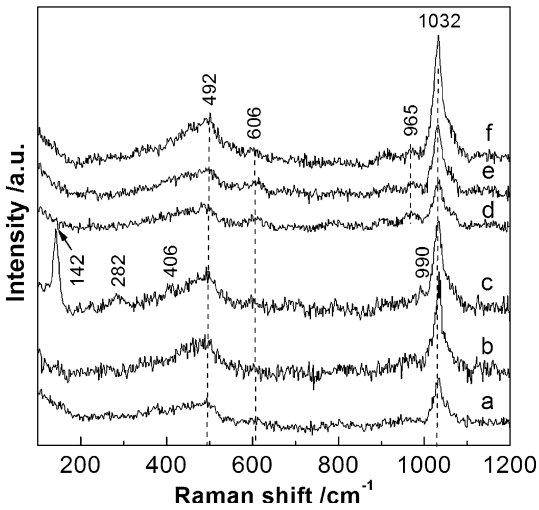

Fig. 3 *In situ* Raman spectra recorded in O_2 flow at 500 °C (50 mL/min). (a) 1.8V/SBA-15; (b, c) 3V/SBA-15; (d) 1.8V-SBA-15; (e) 3V-SBA-15; (f) 3.4V-SBA-15.

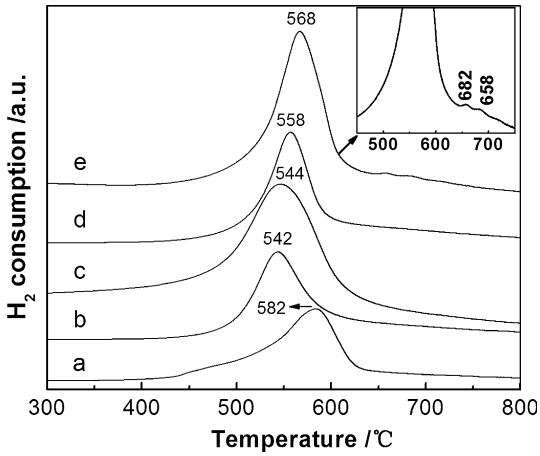

Fig. 4 H2-TPR profiles of the different catalysts. (a) 1.8V/SiO2; (b) 1.8V-SBA-15; (c) 3V-SBA-15; (d) 1.8V/SBA-15; (e) 3V/SBA-15.

3.0% loading. With further increasing V content up to 3.4%, the propane conversion decreases, probably due to the decrease in BET surface area of this sample. It is worth to note that appreciable amount of oxygenates is formed at 500 °C on V-SBA-15 catalysts with low V contents. Remarkable activity for propylene formation is observed at high temperature and high space velocity. The highest propylene yield of 20.3% is attained on 1.8V-SBA-15 catalyst under $T = 600\ ^\circ$ C and GHSV = 25,000 L kg-cat^{-1} h^{-1} conditions, which results in a high space-time yield (STY_{C3H6}) of 3.35 kg propylene per kg-cat^{-1} h^{-1}. It has been pointed out that, generally, an industrially interesting STY_{C3H6} is at least at 1 kg propylene per kg-cat^{-1} h^{-1} [19]. In this work, the STY_{C3H6} obtained with V-SBA-15 catalysts except 0.8V-SBA-15 is well above this value, and close to those with V-MCF catalysts most recently reported [20].

From Table 2, it is also seen that the catalytic performance of the V-SBA-15 catalyst prepared by direct synthesis is superior to those of V/SBA-15 and V/SiO_2 catalysts by impregnation method. On these catalysts with the same V content, propane conversion and TOF value decreases in the order: V-SBA-15 > V/SBA-15 > V/SiO_2, while the propylene selectivities are comparable, indicating that V-SBA-15 is more active for selective oxidation of propane to propylene. Such an activity scale is consistent with the sequence of the surface areas as shown in Table 1. Thus, it is considered that the surface area may be one of the factors affecting the catalytic performance. Larger surface area allows for the higher dispersion of V species, and would result in higher TOF value and higher propane conversion. On the other hand, however, another factor also has to be taken into consideration. For the V-SBA-15 samples prepared by the direct synthesis, a part of V could be incorporated inside the framework of SBA-15. The V species inside the framework are probably less active for propane oxidative dehydrogenation than those on the wall surface, as reported for the V-containing MCM-41 catalysts [21]. This may be one of the reasons why V-SBA-15 and V/SBA-15 show no significant difference in catalytic performance, although their surface areas are quit different.

For the three different V-containing catalysts with the same V content of 3.0 at.%, the variation of the selectivity to propylene with the propane conversion is further compared in figure 5. The results were obtained by changing the flow rate of feed gas at 600 °C. The selectivity to propylene decreases with the propane conversion on all the samples. At the same propane conversion levels, however, it is seen that both 3V-SBA-15 and 3V/SBA-15 show much higher selectivities than 3V/SiO_2. It is also seen that 3V-SBA-15 is slightly more selective as compared with 3V/SBA-15 catalyst. The different selectivities to propylene on the three catalysts could be related to their difference in V dispersion.

Table 2
Oxydative dehydrogenation of propane on the different catalysts[a]

Catalysts	T (° C)	X (C_3H_8) (%)	Selectivity (%)					Y (C_3H_6) (%)	Y (Olefins)[c] (%)	TOF × 10^{20} (μmol C_3H_6at-V^{-1} s^{-1})	STY (C_3H_6)[d] (kg kg-cat^{-1} h^{-1})
			C_3H_6	C_2H_4	Oxygennates[c]	CO	CO_2				
without catalyst	500[b]	~ 0	–	–	–	–	–	–	–	–	0.09
	600	1.6	75.6	14.9	9.6	~ 0	~ 0	1.2	1.4	–	0.20
0.8V-SBA-15	500[b]	7.1	54.4	2.2	22.3	14.6	6.6	3.9	4.0	0.9	0.11
1.8V-SBA-15	500[b]	23.1	39.8	4.1	20.5	23.3	12.3	9.2	10.1	1.0	0.26
	600	48.6	41.8	14.0	1.1	27.0	3.9	20.3	27.1	12.5	3.35
3V-SBA-15	500[b]	26.2	42.9	4.6	7.6	28.2	15.5	11.2	12.4	0.7	0.31
	600	45.1	41.5	10.1	6.3	27.7	8.5	18.7	23.3	6.9	3.09
3.4V-SBA-15	500[b]	24.9	41.7	2.3	7.8	30.3	15.8	10.4	11.0	0.6	0.29
	600	42.6	43.5	9.5	6.4	29.0	6.4	18.6	22.6	6.2	3.08
1.8V/SBA-15	600	45.5	39.2	12.8	5.5	30.0	4.7	17.8	23.7	11.0	2.94
3V/SBA-15	500[b]	25.2	38.4	3.3	4.3	30.0	21.3	9.7	10.5	0.6	0.30
	600	43.3	41.4	9.8	7.2	29.4	5.8	18.0	19.1	6.7	2.97
3V/SiO_2	500[b]	24.9	36.3	0.9	3.3	33.8	22.4	9.0	9.3	0.5	0.25
	600	29.1	41.4	2.0	9.1	27.8	19.3	12.1	12.6	4.5	2.00

[a] Reaction conditions: catalyst, 0.133 g, C_3H_8:O_2:He = 1.2:1.0:1.2, GHSV = 25000 L kg-cat^{-1} h^{-1}.
[b] GHSV = 4200 L kg-cat^{-1} h^{-1}.
[c] Oxygenates, i.e., acrolein and trace acetaldehyde; olefins, i.e., C_3H_6 and C_2H_4.
[d] Space-time yield of propylene.

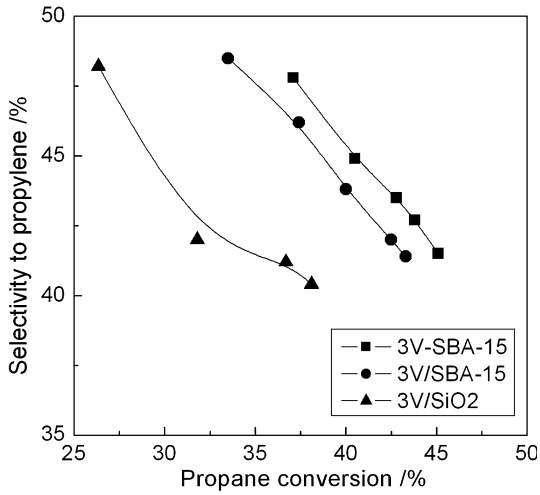

Fig. 5 Variation of the selectivity to propylene with the propane conversion obtained during the oxidation of propane at 600 iæ on 3V-SBA-15, 3V/SBA-15 and 3V/SiO2 catalysts.

Highly dispersed and isolated VO_x species would be favorable to propylene formation.

4. Conclusions

In this work, V-containing SBA-15 mesoporous materials have been directly synthesized through peroxo route. As compared with V/SBA-15 and V/SiO_2 catalysts prepared by impregnation method, the catalyst obtained in this way showed larger surface area, higher V-dispersion and superior catalytic performance for ODH of propane. Moreover, the direct one-pot synthesis of V-containing SBA-15 is more convenient and time-saved than the traditional methods in which lengthy hydrothermal synthesis of SBA-15 is involved.

Acknowledgments

This work was supported by the ministry of Science Technology (2005CB221408, 2005CB221401), the National Natural Science Foundation of China (No. 20433030) and Key Scientific Project of Fujian Province, China (2005HZ01-3).

References

[1] A. Parmaliana, V. Sokolovskii, D. Miceli and N. Giordano, Appl. Catal. A 135 (1996) L1.
[2] A. Corma, J.M. López Nieto and N. Paredes, J. Catal. 144 (1993) 425.
[3] X. Gao, P. Ruiz, Q. Xim, X. Guo and B. Delmon, J. Catal. 148 (1994) 56.
[4] U. Schart, M. Scharmi-Marth, A. Wokaun and A. Baiker, J. Chem. Soc. Faraday Trans. 87 (1991) 4299.
[5] M. Sato, M. Toita, T. Sodesawa and F. Nozaki, Appl. Catal. A 62 (1990) 73.
[6] Liu Y.M., Cao Y., Zhu K.K., Yan S.R., Dai W.L., He H.Y., Fan K.N. (2002) Chem. Commun. 2832.
[7] Y.M. Liu, Y. Cao, S.R. Yan, W.L. Dai and K.N. Fan, Catal. Lett. 88 (2003) 2832.
[8] H.H. Lopez and A. Martinez, Catal. Lett. 83 (2002) 37.
[9] C. Hess, J.D. Hoefelmeyer and T.D. Tilley, J. Phys. Chem. 108 (2004) 9703.
[10] E. Briot, J.-Y. Piquemal and J.-M. Brégeault, N. J. Chem. 26 (2002) 1443.
[11] P.C. Bakala, E. Briot, L. Salles and J.-M. Brégeault, Appl. Catal. A 300 (2006) 91.
[12] D. Zhao, J. Feng, Q. Huo, N. Melosh, G.H. Fredrickson, B.F. Chmelka and G.D. Stucky, Science 279 (1998) 548.

[13] C.J. Brinker, R. Kirkpatrick, D.R. Tallant, B.C. Bunker and B. Montez, J. Non-Cryst. Solids 99 (1988) 418.
[14] S.T. Oyama, G.T. Went, K.B. Lewis, A.T. Bell and G.A. Somorjai, J. Phys. Chem. 93 (1989) 6786.
[15] G.T. Went, S.T. Oyama and A.T. Bell, J. Phys. Chem. 94 (1990) 4240.
[16] I.E. Wachs, F.D. Hardcastle and S.S. Chan, Mater. Res. Soc. Symp. Proc. 111 (1988) 353.
[17] C.-B. Wang, G. Deo and I.E. Wachs, J. Catal. 178 (1998) 640.
[18] F. Arena, F. Frusteri and A. Parmaliana, Appl. Catal. 176 (1999) 189.
[19] J.B. Stelzer, J. Caro and M. Fait, Catal. Commun. 6 (2005) 1.
[20] Y.M. Liu, W.L. Feng, T.C. Li, H.Y. He, W.L. Dai, W. Huang, Y. Cao and K.N. Fan, J. Catal. 239 (2006) 125.
[21] Y. Wang, Q.H. Zhang, Y. Ohishi, T. Shishido and K. Takehira, Catal. Lett. 72 (2001) 215.